

## CRYSTAL-SIZE DEPENDENCE OF ILLITE-SMECTITE ISOTOPE EQUILIBRATION WITH CHANGING FLUIDS

LYNDA B. WILLIAMS\* AND RICHARD L. HERVIG

Department of Geological Sciences, Arizona State University, Tempe, Arizona 85287-1704, USA

**Abstract**—Differences in equilibration rates among crystals of different sizes may be used to deduce paleofluid changes over time if the crystal-growth mechanism is known. To explore isotopic equilibration rates as a function of illite growth, we studied B-isotope changes during illitization of smectite. Montmorillonite (<2.0  $\mu\text{m}$  SWy-1, K saturated) was reacted with aqueous boric acid (1000 ppm B) at 300°C, 100 MPa in sealed Au capsules (1:1 fluid:mineral ratio). The initial fluid was 0‰ (NBS 951 standard) but after R1 ordering occurred (65 days of reaction) the fluid was changed to  $-7\text{‰}$  in order to examine the rate of isotopic re-equilibration. Samples were taken intermittently throughout the experiment. Each aliquot was  $\text{NH}_4$  exchanged and size separated into fine (<0.2  $\mu\text{m}$ ), medium (0.2–2.0  $\mu\text{m}$ ) and coarse (>2.0  $\mu\text{m}$ ) fractions. The isotopic composition of B in the tetrahedral sheet was then measured for comparison with the predicted equilibrium values.

The fine fraction showed equilibrium isotope ratios within 10 days, indicating that small, newly nucleated crystals precipitate in equilibrium with the fluid under supersaturated, closed conditions. These fine-fraction minerals did not re-equilibrate when the fluid was changed. The medium fraction gradually equilibrated with the initial fluid as illite grew to values >50%, but did not re-equilibrate with the later fluid. The coarse fraction was slow to begin recrystallization, perhaps due to dissolution kinetics of large crystals or the presence of detrital contaminants. However, it showed the fastest rate of isotopic change with crystal growth after R1 ordering. We conclude that at 300°C, the initial B–O bonds formed in illite are stable, and isotopic re-equilibration only occurs on new crystal growth. Therefore, different isotope ratios are preserved in different crystal size fractions due to different rates of crystal growth. Large crystals may reflect equilibrium with recent fluid while smaller crystals may retain isotope compositions reflecting equilibrium with earlier fluids.

**Key Words**—Boron, Crystal Growth, Equilibrium, Experimental, Illite-smectite, Isotopes, Reaction Kinetics.

### INTRODUCTION

The crystallization conditions of illite fundamental particles are important for the interpretation of paleofluid chemistry in sedimentary basins (Clauer *et al.*, 2003). In the last decade, studies of crystal-growth mechanisms (Eberl *et al.*, 1998a) and dating of size-separated illite-smectite (I-S) crystals (*e.g.* Pevear, 1992; Clauer *et al.*, 1997; Środoń and Clauer, 2001) from a variety of sedimentary environments have shown that both chemical and physical factors influence illite crystallization and may affect interpretations based on illite chemistry.

Suites of samples from sedimentary basins of different ages and thermal exposure show chemical variations indicating that temperature is the main kinetic factor in illite crystallization (Elliot *et al.*, 1991). However, the effect of fluid and mineral chemistry also influences the reaction kinetics and pathway (Eberl *et al.*, 1978; Roberson and Lahann, 1981; Güven and Huang, 1991). The fluid/mineral ratio and/or pore space available for crystal growth may also influence the crystallization mechanism (Clauer *et al.*, 1999).

Evidence for solid-state transformation (Drits *et al.*, 2002) is often found in environments of low permeability (shales, bentonite), while dissolution/crystallization mechanisms are more obvious in regions of high permeability (sandstone, hydrothermal systems).

The reaction of smectite to illite is one of the most common diagenetic reactions in upper crustal rocks so it is important, although sometimes difficult, to determine if the reaction path varies in different geological environments. One approach is to examine the isotopic changes that occur in B because it substitutes in only one crystallographic site (tetrahedral) of the mineral (Palmer and Swihart, 1996). It is commonly assumed that over geological time, minerals approach equilibrium with the surrounding fluids, and therefore the isotopic composition of a mineral will reflect the temperature and/or isotopic composition of the fluid. This is commonly true for minerals in high-temperature systems (>300°C) where isotopic equilibration occurs in periods of <1 y (Whitney and Northrup, 1988). However, at diagenetic temperatures (60–150°C), isotopic equilibrium may be approached more slowly and must be evaluated in terms of the elemental exchange mechanisms.

Misinterpretations of isotopic information from I-S arise from either detrital impurities, contaminants adsorbed on the high surface area of clay minerals, or

\* E-mail address of corresponding author:

Lynda.Williams@asu.edu

DOI: 10.1346/CCMN.2006.0540501

from the non-equilibrium state of some crystals within a bulk sample. The smectite interlayer region can hold a variety of elements (e.g. O, H, N, B) that are adsorbed (exchanged) from the most recent fluids in contact with the mineral. These elements do not necessarily represent equilibrium isotope ratios that existed when the silicate layers were formed (Marumo *et al.*, 1995; Williams and Hervig, 2002; 2005). For B and Li we have found that the isotopic composition of the bulk I-S (including interlayer species) can be 10–15‰ heavier than the isotopic composition of the silicate framework (Williams and Hervig, 2002). Therefore, depending on which isotopic system is considered, special care must be taken to remove exchangeable elements (ionic or molecular) that could interfere with the silicate isotopic composition. This has been done by dehydration and dehydroxylation for studies of O and H isotopes (Girard and Savin, 1996; Sheppard and Gilg, 1996; Marumo *et al.*, 1995) but can also be done by cation exchange for trace elements such as B and Li (Williams and Hervig, 2005).

The more difficult factor to address when trying to derive paleo-geochemical information from I-S is the problem of isotopic re-equilibration. Many studies (Eberl *et al.*, 1998a; Środoń *et al.*, 2000; Mystkowski *et al.*, 2000; Brime and Eberl, 2002; Bove *et al.*, 2002; Eberl *et al.*, 2002; Kile and Eberl, 2003) have now shown that I-S crystal growth occurs according to the ‘Law of Proportionate Effect’ (Kapteyn, 1905). The crystal-size distributions of natural I-S are most commonly log-normal (Eberl *et al.*, 1998a). This relationship among size fractions can only be retained if crystal growth rates are not identical for all crystals. This important realization led to development of crystal-growth models based on size-dependent growth rates (Eberl *et al.*, 2002). If crystal growth rates depend on crystal size and isotopic exchange occurs by precipitation rather than diffusion (Williams and Hervig, 2005), then a bulk sample of I-S will include a suite of crystals in various stages of re-equilibration with the most recent fluid. Furthermore, it has been shown that in order to maintain a log-normal or asymptotic crystal-size distribution, some crystals that nucleated earlier stop growing entirely (Clauer *et al.*, 1997; Eberl *et al.*, 1998a). This is extremely important for paleofluid reconstruction because the chemistry of those crystals may represent equilibrium with an earlier fluid or at a lower burial temperature. Therefore, if the approach to equilibrium can be sorted out for crystals of different size, then chemical analyses of different sized crystals might reveal the entire paleofluid chemical history in a single rock sample.

In order to test the rate of isotopic equilibration as a function of crystal growth, we conducted a hydrothermal experiment at 300°C (100 MPa) starting with SWy-1 smectite (<2.0 µm fraction) and an aqueous B solution (1000 ppm B), similar to previous experiments where we

determined the equilibrium isotope fractionation of B between illite and water (Williams *et al.*, 2001). However, this time the B-isotope composition of the fluid was changed after R1 ordering of I-S occurred. This was done to examine whether or not isotopic re-equilibration would occur as I-S became more highly ordered (approaching R3). We then separated out different crystal size fractions and measured their respective approach to the equilibrium isotope ratio predicted for 300°C. Here we present the results of this experiment and discuss the potential for determining paleofluid history from different crystal size fractions of illite.

## EXPERIMENTAL DETAILS

The experiment was conducted in sealed Au capsules that were pressurized in a modified cold seal pressure vessel (Williams *et al.*, 2001) using water as a pressurizing medium. The vessel is 54 cm long with a 2 cm inner diameter allowing up to 14 capsules to be loaded within a region confined to a thermal gradient no greater than ±5°C. This was monitored by two internal thermocouples placed at either end of the Au capsules. A Teflon O ring that would normally fail at temperatures above 200°C seals the pressure vessel; therefore cooling fins were used help to cool the sealing head to no more than 50°C. This modification was made in order to quench the experiment more rapidly, remove a capsule, and get the remaining capsules back to experimental conditions as quickly as possible.

The Au capsules were annealed at 550°C overnight, and then cooled for loading. The reaction material was the reference mineral SWy-1 montmorillonite (from The Clay Minerals Society’s Source Clays Repository, Purdue, Indiana) prepared by K saturating with 1 N KCl for 24 h, removing the Cl<sup>-</sup> by dialysis until the exchange water showed no precipitation when AgNO<sub>3</sub> was added, and then separating the <2.0 µm size fraction by centrifugation. Potassium saturation was chosen in order to promote illitization under hydrothermal conditions (Whitney and Northrup, 1988). The B-isotopic composition of this size fraction was -3.0±0.3‰ and contained 10 ppm B after K saturation. The clay was then dried at 60°C and an aliquot of 200 mg was placed in each of 10 capsules. An equivalent weight of B solution was added to the dried, weighed minerals in the capsule. The initial solution contained 1000 ppm B from the NIST SRM 951 boric acid standard, which is the isotopic reference for B, therefore the δ<sup>11</sup>B was 0‰.

The closed end of the capsules was immersed in an ice bath during arc welding to seal the capsules. Capsules were weighed carefully before and after welding them shut to ensure no water loss due to evaporation. The seal was tested by heating the capsules to 100°C for 10 min and checking for weight loss. If no vapor had escaped, the capsules were loaded in the

hydrothermal vessel monitored by two internal thermocouples and a Bourdon tube pressure gauge. The vessel was heated in a Lindburgh clamshell furnace. During heating, a pressure relief valve kept constant pressure at 100 MPa. It took between 1 and 2 h for the experimental run conditions to reach steady state each time the vessel was quenched. Capsules containing the reaction products were removed sequentially at intervals to monitor reaction progress.

After 65 days, all remaining capsules were removed and cut open. The minerals were combined from all capsules, and K exchanged again to remove any B trapped in the interlayers, and to further promote illitization. After dialysis, drying, and reloading of aliquots of the clay into new Au capsules, a new 1000 ppm B solution was added with a  $\delta^{11}\text{B}$  of  $-7\text{‰}$ . We made the solution from a mixture of NBS 952 boric acid (95%  $^{10}\text{B}$  enriched) and a boric acid (99%  $^{11}\text{B}$  enriched) purchased from Cambridge Isotope Laboratories Inc. The experiment was continued for a total of 160 days with the  $-7\text{‰}$  B-solution.

One set of capsules was reacted with only 0‰ boron in water for 240 days without changing fluid, as a control group. In earlier experiments the products reached O-isotopic equilibrium with water at 300°C in 160 days (Williams *et al.*, 2001). We used the O-isotope equilibration (Savin and Lee, 1988) as an indication of the end-point of the illitization reaction, even though only 80% illite was produced. The reaction is limited by supply of Al, as well as K, and therefore did not reach the ideal end-member illite composition. Nonetheless, B-isotope exchange in the tetrahedral sites of the silicate sheet cannot occur without breaking Si–O bonds, therefore when O is at equilibrium, B must be as well.

## METHODS

### *Sample preparation*

The Au capsules were re-weighed after reaction to test for leaking after pressurizing at 100 MPa. If no weight change had occurred, the solid products were removed from the Au capsules using a sterile razor and tweezers to open the capsule wall. The minerals were washed out with 1–2 mL of nominally ‘B-free’ distilled, deionized water that had been filtered through Amberlite resin (Tonarini *et al.*, 1997). It is important to remove adsorbed B contaminants from the clay mineral surface before isotopic analysis (Williams *et al.*, 2001). Hingston (1964) showed that mannitol, a polyhydric alcohol that strongly bonds B to the OH groups, effectively removes adsorbed B from exterior clay surfaces. Therefore, 10 mL of 1.82% mannitol solution (Tonarini *et al.*, 1997) was used to wash the clay products. The minerals were disaggregated using a Branson Ultrasonifier, and then shaken for two or more hours in a wrist-action shaker. Finally, mannitol was washed from the sample by centrifugation, in triplicate,

using ‘B-free’ water. An aliquot of this sample containing ‘Bulk-B’ was mounted for solid-state isotope analysis. The remainder was  $\text{NH}_4$  exchanged to re-expand the smectite and remove interlayer B (Zhang *et al.*, 1998). This treatment has been shown to work as well as divalent cation exchange treatments (Williams and Hervig, 2005), and effectively removes the interlayer B leaving only B substituting in the tetrahedral sheets. After  $\text{NH}_4$  exchange, the samples were size separated by centrifugation into fine ( $<0.2\ \mu\text{m}$ ), medium ( $0.2\text{--}2.0\ \mu\text{m}$ ) and coarse ( $>2.0\ \mu\text{m}$ ) fractions.

### *X-ray diffraction*

X-ray diffraction (XRD) was used to determine the %illite formed over time. The standard ‘glass slide’ sample preparation method (Moore and Reynolds, 1997) was used for oriented clay mounts but as the amount of material was small, the minerals were mounted on quartz slides with no background diffraction peaks. Oriented clay samples were treated with ethylene glycol to expand smectite interlayers. A Siemens D-5000 spectrometer with  $\text{CuK}\alpha$  radiation was used for analysis.

For crystal-size distribution analysis, the end-products after 160 days of reaction, were treated with 10,000 Dalton polyvinylpyrrolidone (PVP-10) according to the procedure described by Eberl *et al.*, (1998b). The expandable smectite layers are eliminated by Na saturating and replacing the interlayer with the high molecular weight PVP-10. This essentially isolates the newly crystallized illite particles so that their thickness can be measured by XRD peak broadening. The XRD patterns were interpreted using the Mudmaster and Galoper programs (Eberl *et al.*, 1996, 2000, respectively) that calculate the crystal-size distribution and growth mechanism (constant nucleation *vs.* surface- or supply-controlled growth).

### *Secondary ion mass spectrometry*

Samples were prepared for solid-state isotope analyses using a Cameca 3f Secondary Ion Mass Spectrometer (SIMS). The size-separated clay fractions were dropped in suspension onto a B-free glass slide. A 5  $\mu\text{L}$  drop contains enough material (few mg) for hundreds of analyses. The only requirement is that the samples are flat, and because clays generally dry flat from suspension, they are ideal for SIMS analysis. Several samples can be mounted on a 25 mm diameter round slide, with the standard reference material mounted in the center. After drying at room temperature, the samples were coated with Au to alleviate charge build-up, and analyzed in a vacuum ( $<10^{-7}$  Torr). For B-isotope analysis we used an  $\text{O}^-$  primary ion beam accelerated to 12,500 V, and focused onto the sample held at +4500 V so that the total impact energy is  $\sim 17,000$  V. The energy of primary ion impact breaks bonds on the mineral surface releasing atoms and ions from a crater that during the course of analysis reaches a

depth of 2–3  $\mu\text{m}$ . The diameter of the crater is determined by the primary beam intensity and focus. For high-resolution isotope analyses the beam can be focused to <10  $\mu\text{m}$ , but as our clay samples are already separated and purified, the lateral resolution is unimportant. Therefore we defocused the beam to  $\sim 30 \mu\text{m}$  to average more clay-sized particles in the analyzed area, and to 'sputter' the crater at a slower rate, yielding a more stable secondary current.

The ions sputtered from the sample by the primary beam bombardment are accelerated through an electrostatic analyzer, and then enter a secondary magnet where they are separated by mass. By adjusting the entrance and exit slits on the mass spectrometer, we can increase the mass resolving power ( $M/\Delta M$ ) to exclude interfering species (Figure 1). For a B-isotope ratio measurement we count the more abundant mass  $^{11}\text{B}$  for 2 s and the less abundant mass  $^{10}\text{B}$  for 8 s since it is four times less abundant than  $^{11}\text{B}$ . The ratios are collected iteratively for 99 cycles and averaged for the final delta value calculation (defined below). Predicted analytical errors (PE) are calculated from counting statistics based on total number of counts for each mass (Long, 1995). If the standard error (SE) of the 99 ratios is more than twice the PE, the analysis is rejected. Typically we average between 5 and 20 analyses on different spots of each sample. A standard is measured in between each sample in order to detect and correct any instrumental drift. Our internal standard reference material is <2.0  $\mu\text{m}$  IMt-1 (Silver Hill illite) that was analyzed by thermal ionization mass spectrometry (in two different labs) and has an average value of  $-9.1 \pm 0.6$  ( $n = 5$ ) relative to the NIST standard for B-isotope ratio measurements NBS SRM 951 boric acid ( $^{11}\text{B}/^{10}\text{B} = 4.0437$ ). A typical error in SIMS measurements on this standard is  $\pm 0.8\%$  over 15 analyses. Measurement of the standard allows us to determine the instrumental mass fractionation (IMF)

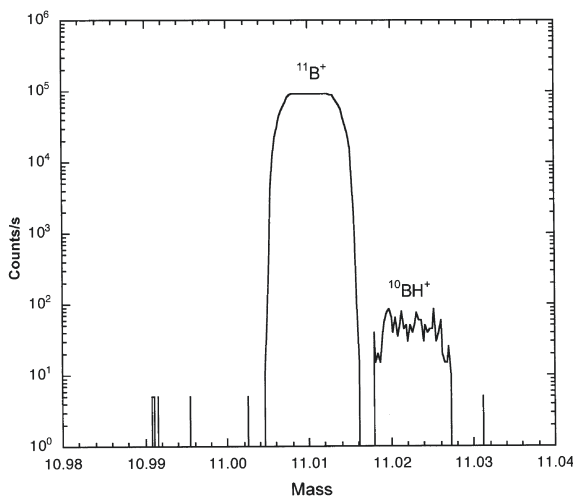


Figure 1. High-resolution mass spectrum showing clear separation of  $^{11}\text{B}$  from the interfering hydride. At these conditions,  $^{10}\text{B}^+$  is also separated from potential interfering species.

for each analytical session, which varies due to small changes in beam alignment and instrument electronics over time. The IMF for B isotopes does not vary by more than a few per mil during an analytical session, and is generally between  $-30$  and  $-40\%$ . This correction is applied to the delta value calculation defined by:

$$\delta^{11}\text{B}\text{‰} = \left[ \left( \frac{^{11}\text{B}/^{10}\text{B}_{\text{sample}}}{^{11}\text{B}/^{10}\text{B}_{\text{NBS 951}}} - 1 \right) \times 1000 \right] - \text{IMF}$$

The B content of clay samples is estimated using a calibration curve determined on minerals and glasses of known B and silica content (Hervig, 1996). The ratio of  $^{11}\text{B}^+ / ^{30}\text{Si}^+$  is measured, and B content is calculated as:

$$\text{B (ppm)} = ^{11}\text{B}/^{30}\text{Si} \times \text{SiO}_2 \text{ (wt. fraction)} \times 10,000$$

Multiple analyses of samples with B contents in the range 10–100 ppm indicate that errors in concentration are <5%.

## RESULTS

### Mineralogical

*X-ray diffraction.* The XRD patterns of representative experimental run products demonstrate mineralogical changes over time (Figure 2). The initial SWy-1 smectite is randomly ordered, with a peak near  $5^\circ 2\theta$ . R1 ordering of I-S begins as this peak shifts to  $6^\circ 2\theta$  and this is observed in the day 37 and day 50 products, although there appears to be unreacted smectite remaining as well. Long-range ordering is indicated when there is a shift of this peak to between  $7$  and  $8^\circ 2\theta$  (Moore and Reynolds, 1997). We observe a shift to  $7.3^\circ 2\theta$  by day 80, indicating R > 1 ordering. The more highly ordered samples all contained a small amount of chlorite and silica (qtz). The reaction progress is similar to our previous experiments where SWy-1 (<2.0  $\mu\text{m}$ ) starting material was used (Williams *et al.*, 2001). Figure 3 shows the %illite formed over time, as interpreted by the  $\Delta 2\theta$  method (Moore and Reynolds, 1997). Clearly, at  $300^\circ\text{C}$  the most rapid illitization occurs in the first month of reaction progress as 50–60% illite is produced. Reaction progress slows during R1 ordering with <10% additional illite produced. There is a jump in the illitization coincident with addition of  $\text{K}^+$  when the samples were K saturated on day 65 coincident with the change in fluid  $\delta^{11}\text{B}$ . The final I-S products contained  $\sim 80\%$  illite.

*Crystal-size distribution.* The crystal-size distribution (CSD) of the day 160 reaction products was analyzed using the program Mudmaster (Eberl *et al.*, 1996). The results (Figure 4) show a log normal distribution with a mean particle size of 4.2 nm. Although these small particles could not be separated by our centrifuge methods, this population makes up a significant portion of the <0.2  $\mu\text{m}$  fraction that was isolated. The natural logarithms of the CSD mean ( $\alpha$ ) and variance ( $\beta^2$ ) are

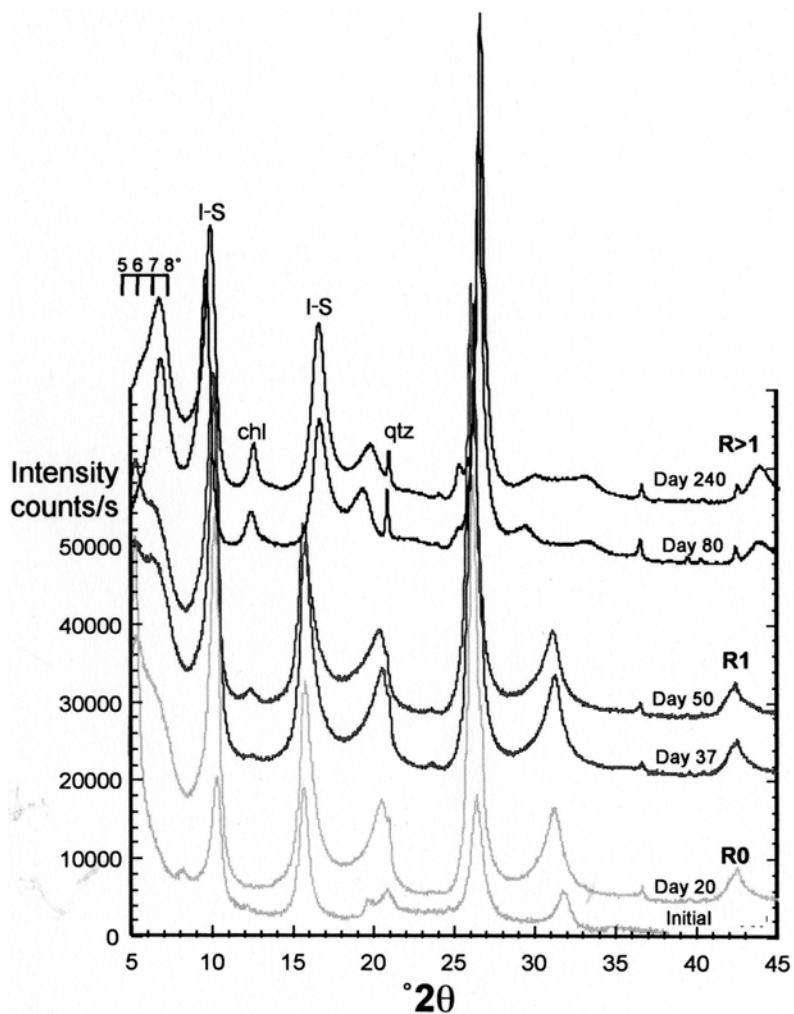


Figure 2. XRD patterns of selected bulk clay products treated with ethylene glycol to demonstrate the reaction of smectite to illite over 240 days. Ordering of I-S is indicated by shifts in the low-angle peaks between 5 and 8°2θ.

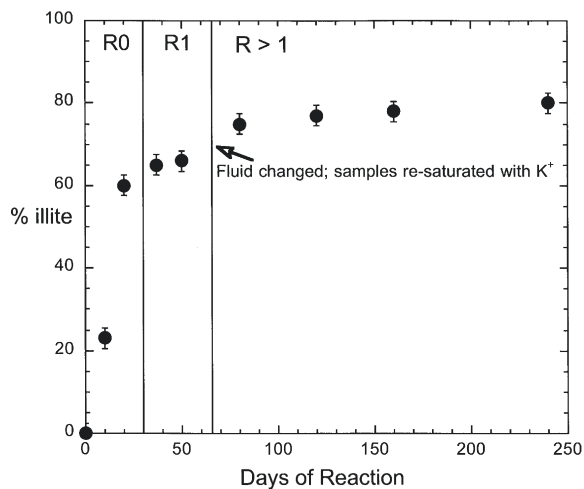


Figure 3. Percent illite estimated from the  $\Delta 2\theta$  method (Moore and Reynolds, 1997) showing slow illitization after 65 days when the isotopic composition of the fluid was changed.

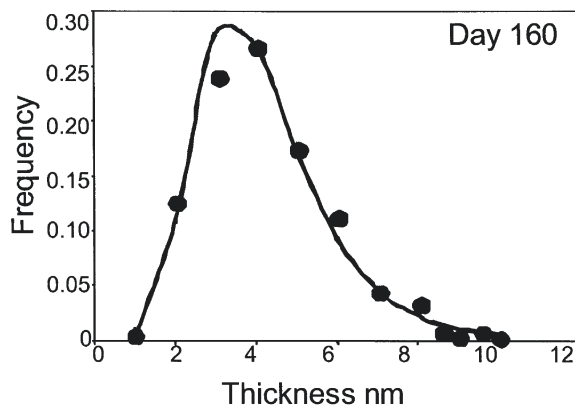


Figure 4. Results of crystal-size distribution using the Mudmaster (Eberl *et al.*, 1996) model (line) compared with XRD measurements (dots).

Table 1. B content [B] (ppm) and isotope ratios (‰) of reaction products. The bulk samples were washed in mannitol, removing exterior adsorbed B. The size-separated samples were NH<sub>4</sub> exchanged to remove interlayer B. Size fractions studied were <0.2 μm (fine), 0.2–2.0 μm (medium) and >2.0 μm (coarse). The starting material was <2.0 μm SWy-1 smectite with 12 ppm B and δ<sup>11</sup>B of -3±0.3‰.

| Day  | Bulk [B] | Bulk δ <sup>11</sup> B | 1σ error | n | Fine [B] | Fine δ <sup>11</sup> B | 1σ error | n  | Medium [B] | Medium δ <sup>11</sup> B | 1σ error | n  | Coarse [B] | Coarse δ <sup>11</sup> B | 1σ error | n  |
|------|----------|------------------------|----------|---|----------|------------------------|----------|----|------------|--------------------------|----------|----|------------|--------------------------|----------|----|
| 10+  | 20       | 1.1                    | 1.0      | 4 | 23       | -14.4                  | 0.5      | 4  | 22         | -10                      | 1.3      | 5  | 19         | -7.3                     | 0.5      | 10 |
| 20+  | 52       | -4.6                   | 0.4      | 3 | 27       | -13.5                  | 0.6      | 4  | 24         | -8.4                     | 0.4      | 3  | 25         | -6.6                     | 0.6      | 3  |
| 37+  | 43       | -1.9                   | 1.0      | 3 | 28       | -17.4                  | 0.5      | 4  | 20         | -15.8                    | 0.6      | 14 | 20         | -6.9                     | 0.8      | 6  |
| 50+  | 38       | -3.2                   | 0.8      | 5 | 24       | -15.7                  | 1.7      | 3  | 20         | -13.5                    | 1.1      | 3  | 20         | -6.6                     | 0.5      | 5  |
| 80-  | 44       | -15.9                  | 1.5      | 5 | 31       | -15.7                  | 0.6      | 10 | 28         | -16.1                    | 1.8      | 3  | 16         | -10.8                    | 0.7      | 3  |
| 120- | 29       | -15.6                  | 0.6      | 3 | 35       | -17.2                  | 0.3      | 15 | 32         | -15.6                    | 1.5      | 3  | 25         | -12.8                    | 0.7      | 9  |
| 160- | 42       | -11.7                  | 0.5      | 3 | 27       | -17.5                  | 0.4      | 3  | 29         | -16.6                    | 0.5      | 3  | 19         | -17.1                    | 1.1      | 7  |
| 160+ | 39       | -12.6                  | 0.4      | 3 | 23       | -17.7                  | 0.5      | 3  | 23         | -15.2                    | 0.6      | 3  | 24         | -7.3                     | 1.3      | 6  |
| 240+ | 29       | -12.1                  | 0.5      | 4 | 32       | -14.5                  | 0.5      | 6  | 25         | -13.1                    | 0.5      | 7  | 25         | -6.4                     | 0.9      | 19 |

+ denotes reaction with 0‰ water only

- denotes reaction with -7‰ water after 65 days of reaction in 0‰ fluid

n is the number of spots analyzed on each sample

1.37 and 0.14, respectively. According to studies of natural illite samples from shales (Brime and Eberl, 2002) these parameters indicate a growth mechanism by surface- or supply-controlled growth. Modeling of crystal growth using the Galoper program (Eberl, 2000) indicated that after the initial nucleation of small crystals, growth was surface- and supply-controlled (D. Eberl, pers. comm.).

#### Chemical

The <2.0 μm fraction of the SWy-1 starting material contains 10 ppm B with an isotope ratio of -3±0.3‰ (Williams *et al.*, 2001). Tests of cation exchange with K<sup>+</sup>, NH<sub>4</sub><sup>+</sup> and Mg<sup>2+</sup> did not show any change in the

measured B content or isotope ratio of the SWy-1 suggesting that negligible B was initially adsorbed in the interlayer. Table 1 shows the B content and isotope composition of the I-S reaction products before and after removal of interlayer B by NH<sub>4</sub> exchange.

**B content.** The amount of 'Bulk B' in the samples (containing interlayer and tetrahedral sheet B) reaches a maximum during R1 ordering (Figure 5, filled circles), but declines during R > 1 ordering, as observed in similar experiments (Williams *et al.*, 2001). The tetrahedral B content (NH<sub>4</sub>-exchanged samples, open circles) of the fine fraction is plotted for comparison. The fine fraction contains the smallest amount of detrital contaminants and therefore best demonstrates the trend for B substitution in the authigenic products. The tetrahedral B content gradually increases during reaction progress and reaches the same steady-state maximum of ~30 ppm as observed in previous experiments (Williams *et al.*, 2001). In general the fine fraction contains more B than the coarser fractions (Table 1).

**B isotopes.** After NH<sub>4</sub> exchange removed interlayer B, the isotopic compositions of the reaction products were analyzed on different size fractions. Figure 6 shows the results for all of the samples separated into fine (<0.2 μm) medium (0.2–2.0 μm) and coarse (>2.0 μm) fractions. Results from the control samples reacted for 240 days with only 0‰ water are shown (Figure 6a) for comparison to the products from capsules where the fluid isotope composition was changed on day 65 (Figure 6b). The experimentally derived fractionation equation for B (Hervig *et al.*, 2002):

$$1000\ln\alpha_{IV-III} = 5.68 - (12,290/T(K))$$

was used to predict the equilibrium fractionation value for tetrahedral B (IV) in the mineral, from a fluid

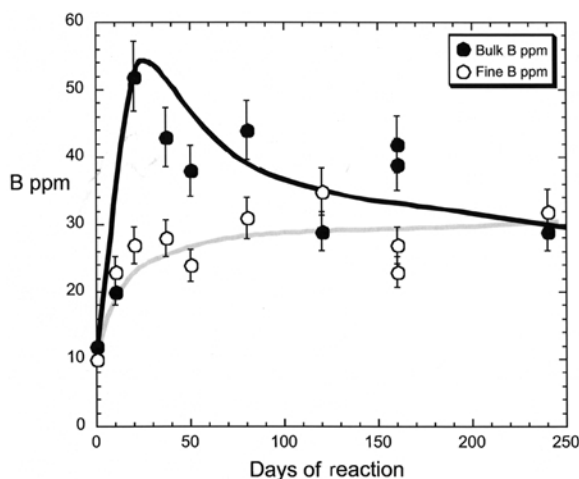


Figure 5. B content of the bulk (filled circles) and fine fraction I-S after removal of interlayer B by NH<sub>4</sub> exchange (open circles). The trend is similar to earlier experiments, showing an increase in interlayer B during R1 ordering, and a decline as long-range ordering occurs. Tetrahedral B shows a gradual increase to steady state.

containing B predominantly in trigonal (III) coordination (e.g. boric acid). Boric acid is the dominant aqueous species of B at low pH (<7; Palmer and Swihart, 1996; Hemming and Hanson, 1992) and the pH of the B solution was 6–6.5 after quench (Williams, 2000); therefore the isotope fractionation between mineral and water is essentially that expected for a tetrahedral–trigonal coordination change. The predicted fractionation value ( $\Delta$ ) at 300°C is  $-16 \pm 2\%$  ( $2\sigma$ ) (Williams *et al.*, 2001).

The fine size fraction approached the predicted equilibrium B-isotope composition after only 10 days of reaction. The medium size fraction gradually approached the predicted equilibrium value over 50 days of reaction. The coarse fraction never reached the predicted isotopic equilibrium value with the 0‰ fluid. There is a slight increase in the fine and medium-sized fractions in the sample from 240 days, which was re-analyzed after an additional  $\text{NH}_4$  exchange to test for incomplete interlayer B removal. These values were reconfirmed.

When the fluid isotope composition was changed to a more negative value ( $-7\%$ ) after 65 days of reaction (Figure 6b), there was no statistical deviation in the isotope ratios of the fine and medium-sized fractions. They retained the isotopic composition from the initial fluid, even after nearly 100 days of exposure to the new fluid. However, the coarse fraction began to show progress toward re-equilibration with the new fluid as indicated by the gradual decline in isotope composition with reaction progress from day 80 to 160.

## DISCUSSION

It is essential to recognize that bulk isotopic analyses of B in expandable clay minerals contain a significant component of interlayer B that must be removed. We have used  $\text{NH}_4$  exchange to achieve this, but other preferred exchange cations or alkylammonium complexes might work as well. This leaves only B bound in tetrahedral sites of the silicate framework. The day 37 reaction products (Figure 7) ideally demonstrate this point. The  $\delta^{11}\text{B}$  of the bulk clay is always more positive than the isotopic composition of B substituted in the tetrahedral sheet, due to preference of  $^{10}\text{B}$  for tetrahedral coordination (Palmer and Swihart, 1996). The water in the interlayer contains more  $^{11}\text{B}$ , preferred in trigonal coordination. Our interest is in the B isotopic composition of the new illite crystals formed in equilibrium with the water; therefore we focus on the isotopic composition of the tetrahedral sheet rather than the ‘bulk clay’ that can trap aqueous  $^{11}\text{B}$ . Figure 6 demonstrates that there are significant differences in the B-isotope composition of different crystal size fractions. Below we discuss our interpretation of the observed B-isotope trends as a function of crystal growth and mechanism of isotopic equilibration.

If illite crystals nucleate and grow at a constant rate, then one would expect the rate of isotopic equilibration to be the same for each crystal size fraction. However, our isotopic data (Figure 6b) show important differences in the rate of equilibration with crystal size. According to the Law of Proportionate growth (Eberl *et al.*, 1998a), small crystals grow more slowly than large crystals, producing the log-normal crystal-size distribution shown for our experiment end-products (Figure 4). However, during  $\text{R0} \rightarrow \text{R1}$  ordering, the smallest size fraction equilibrates most rapidly in our experiment, which seems contradictory to proportionate growth. This can be explained by the conditions of the experiment which, unlike natural environments, rapidly threw the clay into a closed system supersaturated with components that allowed nucleation of abundant fine illite crystals during the first 65 days of reaction (Figure 6b). These fine illite crystals nucleated in isotopic equilibrium with the fluid. Isotopic equilibration is different for the case of constant

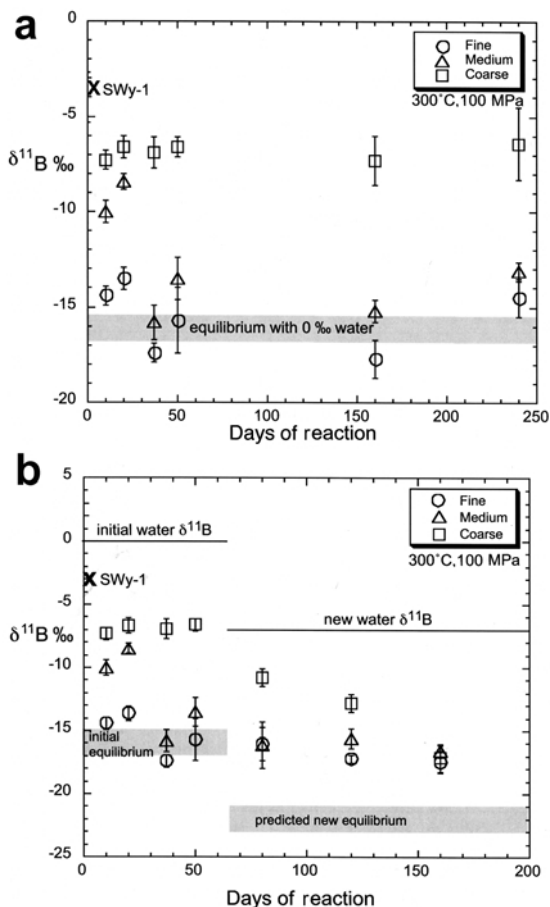


Figure 6. B isotope ratios of reaction products over time. Part a shows the control samples reacted only with 0‰ water containing 1000 ppm B. Part b shows results when water is changed to  $-7\%$   $\delta^{11}\text{B}$  after 65 days. The reaction products were separated into fine ( $<0.2 \mu\text{m}$ ), medium ( $0.2\text{--}2.0 \mu\text{m}$ ) and coarse ( $>2.0 \mu\text{m}$ ) fractions as reported in Table 1. Error bars shown are  $1\sigma$ .

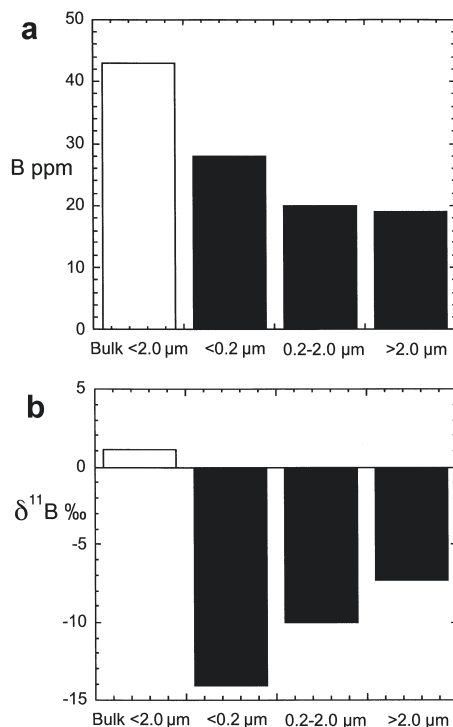


Figure 7. (a) B content and (b) B isotope composition of the day 37 sample. Bulk (interlayer + tetrahedral B) values (white bars) are compared to tetrahedral B only (black bars). Significant differences are observed among different size fractions.

nucleation from a saturated solution, than it would be for the case of surface-controlled growth, due to inherited isotopic ratios. This is why the crystal-growth mechanism must be understood for a given population of clay crystals.

The most frequent crystal size in the <0.2 μm clay fraction is 4.2 nm according to the X-ray peak broadening (Figure 4). Although the XRD data cannot resolve a difference in %illite among the different sized fractions of the products, the differences in measured isotope ratios demonstrate that the fine fraction in our experiment is composed primarily of illite crystals approaching equilibrium with the initial fluid.

Immediate nucleation of small illite crystals results from the abundant supply of reactants that dissolve when the smectite is heated to 300°C. In closed systems, the kinetics of smectite dissolution control the rate of illitization (Eberl *et al.*, 1998a). It follows that the new illite layers forming within the smectite interlayer precipitate in equilibrium with the fluid within a matrix of smectite that remains out of equilibrium. The rate of whole I-S isotope equilibration therefore must depend on the proportion of illite (by volume) within the matrix of smectite. This includes the area (*a-b* dimension) of the illite crystals as well as the %I layers in I-S (*c* dimension).

The medium and coarse size fractions started out as predominantly smectite, with minor detrital phases. Dissolution of the smectite and detrital components provides the Al and K that produces illite by gradual ordering ( $R_0, R_1, R > 1$ ) as indicated by XRD patterns of ethylene glycolated products (Figure 2). The isotopic data show that the medium-sized I-S approached the predicted equilibrium (within error) with the initial 0% water during R1 ordering (by day 50). Over this same time interval, the coarse fraction changed by a small amount (from -3 to -7‰), but never approached the predicted equilibrium value. This may be due to the slower kinetics of dissolution of coarse particles. Alternatively it may be due to the greater amount of detrital components in the coarse material than in the finer sized fractions (Whitney and Northrup, 1988), essentially diluting the isotope ratio of the coarse fraction with non-equilibrium B.

Reaction of <2.0 μm SWy-1 at 300°C for 65 days produced R3 ordered I-S in previous experiments (Williams *et al.*, 2001; Whitney and Northrup, 1988); however  $R > 1$  I-S was produced in this experiment by day 80, and never progressed to R3. This might be due to minor variation in the mineral reactants selected by size fractionation of the bulk clay standard. Changing fluids at day 65 might also have impeded reaction progress if dissolved Al was removed with the initial fluid. Nonetheless, by changing the fluid δ<sup>11</sup>B to -7‰ after 65 days, we tested the potential for the R1 I-S to re-equilibrate during long-range ordering ( $R > 1$ ) in the presence of a new fluid, just as one might encounter in natural sedimentary basins. We observe a notable decline in the isotope ratio of the coarse fraction toward the predicted equilibrium isotope ratio, yet no change in the isotope ratio of the fine and medium-sized fractions.

This trend suggests that the coarse fraction, although slow to re-equilibrate with the first fluid, is growing at a faster rate than the fine and medium size fractions after day 65. The fine fraction contained newly nucleated crystals in equilibrium with the initial fluid, and the medium sized fraction slowly equilibrated with the initial fluid as more illite layers formed in the smectite matrix. The lack of re-equilibration of the fine and medium size fractions with the new fluid indicates that they are either no longer growing, or are growing at a slower rate than the coarse fraction. None of the products reached the predicted isotopic equilibrium by day 160, after nearly 100 days of reaction with the new fluid. We suggest that this is because illite growth was supply limited or surface controlled, and isotopic exchange only occurs during new illite growth.

## CONCLUSIONS

The reactant supply and mineral surfaces predominantly control the rate of crystal growth and approach to isotopic equilibration. The B-isotope trends shown for

different size fractions, and the response of the I-S to fluid change after R1 ordering clearly demonstrate that the small illite crystals retain the equilibrium isotopic composition achieved during early crystallization. Larger size fractions equilibrate more slowly, because they require dissolution of smectite as illite precipitates in interlayer sites (surface- and supply-controlled). The coarsest fraction shows progress toward re-equilibration with the new fluid and would eventually equilibrate if not supply limited.

The differences in growth rate of the different sized crystals provide the potential for an I-S rich sample to record paleofluid chemical or temperature changes over time. If the natural system is closed (e.g. bentonite), and changes in the fluid chemistry are unlikely, then changes in the isotope composition might be used to deduce the temperature of crystallization. However, because crystal growth mechanisms depend on the saturation state of the water (with respect to illite components), the timing of crystal nucleation remains unknown unless the different size fractions are dated. K-Ar dates of illite crystals in different size fractions are a robust tool for evaluating crystal ages and that method is supported by our experiment indicating that illite is not prone to exchange after precipitation at diagenetic temperatures. The different crystals of illite within a single sample of I-S rich clay could therefore record the history of paleofluid changes in a sedimentary basin.

#### ACKNOWLEDGMENTS

We gratefully acknowledge support from the National Science Foundation (EAR 0229583), and the use of facilities in the Center for Solid State Science at Arizona State University. Dennis Eberl (U.S. Geological Survey, Boulder, CO) analyzed the crystal size distributions and we thank him for insightful discussions on crystal growth mechanisms that may influence isotopic equilibration.

#### REFERENCES

- Bove, D.J., Eberl, D.D., McCarty, D.K. and Meeker, G.P. (2002) Characterization and modeling of illite crystal particles and growth mechanisms in a zoned hydrothermal deposit, Lake City, Colorado. *American Mineralogist*, **87**, 1546–1556.
- Brime, C. and Eberl, D.D. (2002) Growth mechanisms of low-grade illites based on shapes of crystal thickness distributions. *Swiss Bulletin of Mineralogy and Petrology*, **82**, 203–209.
- Clauer, N., Środoń, J., Franců, J. and Šuchá, V. (1997) K-Ar dating of illite fundamental particles separated from illite-smectite. *Clay Minerals*, **32**, 181–196.
- Clauer, N., Rinckenback, T., Weber, F., Sommer, F., Chaudhuri, S. and O'Neil, J.R. (1999) Diagenetic evolution of clay minerals in oil-bearing Neogene sandstones and associated shales from Mahakam Delta Basin (Kalimantan, Indonesia). *American Association of Petroleum Geologists Bulletin*, **83**, 62–87.
- Clauer, N., Liewig, N., Pierret, M.-C. and Toulkeridis, T. (2003) Crystallization conditions of fundamental particles from mixed-layer illite-smectite of bentonites based on isotopic data (K-Ar, Rb-Sr and  $\delta^{18}\text{O}$ ). *Clays and Clay Minerals*, **51**, 664–674.
- Drits, V.A., Sakharov, B.A., Dainyak, L.G., Salyn, A.L. and Lindgreen, H. (2002) Structural and chemical heterogeneity of illite-smectites from Upper Jurassic mudstones of east Greenland related to volcanic and weathered parent rocks. *American Mineralogist*, **87**, 1590–1607.
- Eberl, D.D., Whitney, G. and Khoury, H. (1978) Hydrothermal reactivity of smectite. *American Mineralogist*, **63**, 401–409.
- Eberl, D.D., Drits, V.A., Środoń, J. and Nüesch, R. (1996) *MUDMASTER: a program for calculating crystallite size distributions and strain from the shapes of X-ray diffraction peaks*. US Geological Survey Open File Report 96–171.
- Eberl, D.D., Drits, V.A. and Środoń, J. (1998a) Deducing the growth mechanisms of minerals from the shapes of crystal size distributions. *American Journal of Science*, **298**, 499–533.
- Eberl, D.D., Nüesch, R., Šuchá, V. and Tsipursky, S. (1998b) Measurement of fundamental illite particle thicknesses by X-ray diffraction using PVP-10 intercalation. *Clays and Clay Minerals*, **46**, 89–97.
- Eberl, D.D., Drits, V.A. and Środoń, J. (2000) *User's guide to GALOPER – a program for simulating the shapes of crystal size distributions*. US Geological Survey Open File Report 00–505.
- Eberl, D.D., Kile, D.E. and Drits, V.A. (2002) On geological interpretations of crystal size distributions: constant versus proportionate growth. *American Mineralogist*, **87**, 1235–1241.
- Elliott, W.C., Aronson, J.L., Matisoff, G. and Gautier, D.L. (1991) Kinetics of the smectite to illite transformation in the Denver Basin: Clay mineral, K-Ar data and mathematical model results. *American Association of Petroleum Geologists Bulletin*, **75**, 436–462.
- Girard, J.-P. and Savin, S.M. (1996) Intracrystalline fractionation of oxygen isotopes between hydroxyl and non-hydroxyl sites in kaolinite measured by thermal dehydroxylation and partial fluorination. *Geochimica et Cosmochimica Acta*, **60**, 469–487.
- Güven, N. and Huang, W.-L. (1991) Effects of octahedral  $\text{Mg}^{2+}$  and  $\text{Fe}^{3+}$  substitutions on hydrothermal illitization reactions. *Clays and Clay Minerals*, **39**, 387–399.
- Hemming, N.G. and Hanson, G.N. (1992) Boron isotopic composition and concentration in modern marine carbonates. *Geochimica et Cosmochimica Acta*, **56**, 537–543.
- Hervig, R.L. (1996) Analyses of geological materials for boron by secondary ion mass spectrometry. Pp. 789–803 in: *Boron Mineralogy, Petrology and Geochemistry* (E.S. Grew and L.M. Anovitz, editors). Reviews in Mineralogy, **33**, Mineralogical Society of America, Washington, D.C.
- Hervig, R.L., Moore, G.M., Williams, L.B., Peacock, S.M., Holloway, J.R. and Roggensack, K.R. (2002) Isotopic and elemental partitioning of boron between hydrous fluid and silicate melt. *American Mineralogist*, **87**, 769–774.
- Hingston, F.J. (1964) Reactions between boron and clays. *Australian Journal of Soil Research*, **2**, 83–95.
- Kapteyn, J.C. (1903) *Skew Frequency Curves in Biology and Statistics*. Noordhoff Astronomical Laboratory, Groningen, The Netherlands, 69 pp.
- Kile, D. and Eberl, D.D. (2003) On the origin of size-dependent and size-independent crystal growth: Influence of advection and diffusion. *American Mineralogist*, **88**, 1514–1521.
- Long, J.V.P. (1995) Microanalysis from 1950 to the 1990s. Pp. 1–48 in: *Microprobe Techniques in the Earth Sciences* (P.J. Potts, J.F.W. Bowles, S.J.B. Reed and M.R. Cave, editors). Chapman & Hall, London.
- Marumo, K., Longstaffe, F.J. and Matsubaya, O. (1995) Stable isotope geochemistry of clay minerals from fossil and active hydrothermal systems, southwestern Hokkaido, Japan.

- Geochimica et Cosmochimica Acta*, **59**, 2545–2559.
- Moore, D.M. and Reynolds, R.C. (1997) *X-ray Diffraction and the Identification and Analysis of Clay Minerals*, 2<sup>nd</sup> edition. Oxford University Press, New York, 378 pp.
- Mystkowski, K., Środoń, J. and Elsass, F. (2000) Mean thickness and thickness distribution of smectite crystallites. *Clay Minerals*, **35**, 545–557.
- Palmer, M.R. and Swihart, G.H. (1996) Boron isotope geochemistry: an overview. Pp. 709–744 in: *Boron Mineralogy, Petrology and Geochemistry* (E.S. Grew and L.M. Anovitz, editors). Reviews in Mineralogy **33**, Mineralogical Society of America, Washington, D.C.
- Pevear, D.R. (1992) Illite age analysis, a new tool for basin thermal analysis. Pp. 1251–1254 in: *Water-Rock Interaction* (Y.K. Kharaka and A.S. Maest, editors). Balkema, Rotterdam, The Netherlands.
- Roberson, H.E. and Lahann, R.W. (1981) Smectite to illite conversion rates; Effects of solution chemistry. *Clays and Clay Minerals*, **29**, 129–135.
- Savin, S.M. and Lee, M. (1988) Isotopic studies of phyllosilicates. Pp. 189–223 in: *Hydrous Phyllosilicates (Exclusive of Micas)* (S.W. Bailey, editor). Reviews in Mineralogy, **19**, Mineralogical Society of America, Washington, D.C.
- Sheppard, S.M.F. and Gilg, H.A. (1996) The stable isotope geochemistry of clay minerals. *Clay Minerals*, **31**, 1–24.
- Środoń, J. and Clauer, N. (2001) Diagenetic history of Lower Palaeozoic sediments in Pomerania (northern Poland), traced across the Teisseyre-Tornquist tectonic zone using mixed-layer illite/smectite. *Clay Minerals*, **36**, 15–27.
- Środoń, J., Eberl, D.D. and Drits, V.A. (2000) Evolution of fundamental particle size during illitization of smectite and implications for reaction mechanism. *Clays and Clay Minerals*, **48**, 446–458.
- Tonarini, S., Pennisi, M. and Leeman, W.P. (1997) Precise boron isotopic analysis of complex silicate (rock) samples using alkali carbonate fusion and ion-exchange separation. *Chemical Geology*, **142**, 129–137.
- Whitney, G. and Northrup, H.R. (1988) Experimental investigation of the smectite to illite reaction: Dual reaction mechanisms and oxygen-isotope systematics. *American Mineralogist*, **73**, 77–90.
- Williams, L.B. (2000) Boron isotope geochemistry during burial diagenesis. PhD thesis, University of Calgary, Alberta, Canada, 168 pp.
- Williams, L.B. and Hervig, R.L. (2002) Intracrystalline boron isotope variations in clay minerals: a potential low-temperature single mineral geothermometer. *American Mineralogist*, **87**, 1564–1570.
- Williams, L.B. and Hervig, R.L. (2005) Lithium and boron isotopes in illite-smectite: The importance of crystal size. *Geochimica et Cosmochimica Acta*, **69**, 5705–5716.
- Williams, L.B., Hervig, R.L., Holloway, J.R. and Hutcheon, I. (2001) Boron isotope geochemistry during diagenesis: Part 1. Experimental determination of fractionation during illitization of smectite. *Geochimica et Cosmochimica Acta*, **65**, 1769–1782.
- Zhang, L., Chan, L.H. and Gieskes, J.M. (1998) Lithium isotope geochemistry of pore waters from Ocean Drilling Program Sites 918 and 919, Irminger Basin. *Geochimica et Cosmochimica Acta*, **62**, 2437–2450.

(Received 30 December 2005; revised 24 April 2006; Ms. 1128; A.E. W. Crawford Elliott)